Temperature Dependence of the Unperturbed Dimensions of Alternating Poly(ethylene-propylene)

A. Zirkel, D. Richter,* and W. Pyckhout-Hintzen

Institut für Festkörperforschung, Forschungszentrum Jülich, Postfach 1913, D-5170 Jülich 1, Germany

L. J. Fetters*

Corporate Research Laboratories, Exxon Research and Engineering Company, Annandale, New Jersey 08801

Received July 11, 1991; Revised Manuscript Received August 23, 1991

ABSTRACT: The unperturbed dimensions of alternating atactic poly(ethylene-propylene) (PEP) have been investigated by small-angle neutron scattering (SANS) over a wide temperature range. The results were compared with an rotational isomeric state (RIS) calculation using the statistical bond parameters of Mark. The PEP samples were prepared by the hydrogenation of essentially 1,4-polyisoprene. Experimental and theoretical results show good agreement as far as low and intermediate temperatures are concerned. Moreover, the temperature coefficient for chain dimensions of $(-1.16 \pm 0.03) \times 10^{-3}$ K^{-1} extracted from the data in the range of 25-180 °C is in good agreement with the value of $(-1 \pm 0.2) \times 10^{-3}$ K^{-1} obtained from measurements in Θ solutions over a smaller temperature range. Above 180 °C, discrepancies emerge between theory and experiment.

Introduction

The rotational isomeric state (RIS) model has proven to be generally successful for the determination of conformation-dependent properties of polymer chains. Poly(ethylene-propylene) (PEP) random copolymers have been evaluated within the framework of the RIS approach.[1-3] Recently, alternating PEP has been studied by Mathur and Mattice.[4] Their calculations were for stereochemical compositions covering the range from racemic (p = 0) through meso (p = 1), where p denotes the probability that any two successive tertiary carbon atoms have the same stereochemistry.

In this work we investigated the temperature dependence of the unperturbed radius of gyration R_g of the PEP chain by small-angle neutron scattering (SANS) in order to test the RIS predictions over as wide a temperature range as feasible, 25-270 °C. The PEP chain was one with p = 0.5 and served as a model since it exhibits a measurable change in R_g with temperature.

Generally, the temperature coefficient of unperturbed chain dimensions, $d \ln \langle R^2 \rangle_0 / dT(\kappa)$, has traditionally been evaluated by measurements of the intrinsic viscosity $[\eta]$ under Θ conditions or in athermal solvents using the methods of Flory and co-workers.[5-7] Relative to the viscometric method, SANS has the ability to follow R_g in the realistic melt environment (and thus eliminate the potential influence of specific solvent effects) over a much wider range of temperatures than is possible in dilute solution. The determination of κ via Θ solvent measurements[8] led to a value of $(-1 \pm 0.2) \times 10^{-3}$ K^{-1} which is in consonance with that of -1.1×10^{-3} K^{-1} from RIS calculations.[1,4] The Θ condition measurements were restricted to six temperatures over the relatively small temperature range of 5-60.9 °C.

The SANS experiments presented here were carried out in the melt where repulsive and attractive interactions are believed to compensate.[9] A fraction of the melt consisted of deuterated chains in order to obtain contrast in the SANS measurements. Three different concentrations of labeled chains were investigated in order to correct for possible residual H-D interactions.

Experimental Section

The PEP samples were prepared by the hydrogenation or deuteration of 1,4-polyisoprene, as previously described.[8,10] During the polymerization of the parent polyisoprene, about 7% of 3,4 additions are produced.[11] This gives rise to an average bond number of 3.86/monomer unit, which was taken into account in the RIS calculations. The weight-average molar masses were determined using a Chromatix KMX-6 low-angle laser light scattering instrument (λ = 633 nm) with tetrahydrofuran as the solvent. The measurements were carried out at 25 °C and yielded 8.38×10^4 g/mol for the protonated PEP and 8.22×10^4 for the deuterated sample. The protonated PEP served as the matrix material for the deuterated target. Previous experiments using a deuterated matrix failed because of its strong coherent scattering. We believe this scattering to arise from air or Ar bubbles (see text below) enclosed in the material. Due to the large coherent scattering length of deuterium, pronounced contrast to the air or Ar bubbles is produced. The contrast is much smaller in the case of the protonated matrix. In order to correct for possible H-D interactions involving a χ parameter different from zero, three concentrations of 6, 4, and 2 wt % or 5.29, 3.57, and 1.77 vol %, respectively, were measured. They are referred to as 6, 4, and 2% samples in this work.

The polydispersities were examined by using a Waters 150 °C size-exclusion chromatograph (SEC) unit having a differential refractometer. The chains were almost monodisperse with $U = M_w/M_n - 1$ being 0.05. The samples were filled in quartz containers under an inert Ar atmosphere to reduce the penetration of oxygen, which could cause degradation at high temperatures. To achieve uniformity and to reduce microbubbles, the samples were heated at 70 °C for about 24 h.

The SANS experiment was performed on the KWS 2 instrument at the FRJ 2 in the Forschungszentrum Jülich. The wavelength was about 7 Å and the wavelength spread $\Delta\lambda/\lambda \approx 20\%$.[12] The collimation can be modified by diaphragms at various positions. The wave vector range ($Q = 4\pi/(\lambda \sin(\theta/2))$, θ = scattering angle) covered at 2- and 8-m collimation was 0.005-0.14 Å^{-1}. The detector consists of two crossed BF_3 counter tubes with a channel width of about 0.8 cm. The data of both tubes were independently calibrated and subsequently averaged. The beam aperture was 8 × 8 mm^2.

If the interaction of H and D species is neglected, the scattering per unit volume from a mixture of deuterated and nondeuter-

0024-9297/92/2225-0954$03.00/0

ated chains is given by[9]

$$\frac{d\Sigma^{-1}}{d\Omega}(Q) = \frac{1}{\Phi_H V_H{}^w \Delta\rho^2 g(Q^2 R_{g_{H,z}}{}^2)} + \frac{1}{\Phi_D V_D{}^w \Delta\rho^2 g(Q^2 R_{g_{D,z}}{}^2)} \quad (1)$$

Here, Φ_H, $R_{g_{H,z}}$, and $V_H{}^w$ and Φ_D, $R_{g_{D,z}}$, and $V_D{}^w$, respectively, denote the volume fractions, z-average radii of gyration, and weight-average chain volumes (cm^3) of protonated and deuterated materials.

$\Delta\rho^2 = [N_A n(b_H - b_D)/\Omega_0]^2$ is the scattering contrast factor; b_H and b_D are the nuclear coherent scattering lengths for hydrogen and deuterium, and n is the number of exchanged hydrogen atoms per monomer. Ω_0 denotes the monomer volume (cm^3/mol). $g(z)$ is the Debye function $g(z) = 2/z^2(\exp(-z) - 1 + z)$ with $z = Q^2R_g{}^2$.

In the Zimm approximation, which is valid in the small Q range, the cross-section is given by

$$\frac{d\Sigma^{-1}}{d\Omega}(Q) = \frac{1}{\Phi_H V_H{}^w \Delta\rho^2}\left(1 + \frac{R_{g_{H,z}}{}^2 Q^2}{3}\right) + \frac{1}{\Phi_D V_D{}^w \Delta\rho^2}\left(1 + \frac{R_{g_{D,z}}{}^2 Q^2}{3}\right) \quad (2)$$

The chain lengths of protonated and deuterated species are slightly different. Hence their molar masses and radii of gyration also differ. Equation 2 is therefore used to estimate the correction which arises from the difference in chain lengths.

We introduce the difference in molar mass by[13]

$$V_H{}^w = V_D{}^w(1 + w) \quad (3)$$

$$V_H{}^z = V_D{}^z(1 + z) \quad (4)$$

and hence

$$R_{g_{H,z}}{}^2 = R_{g_{D,z}}{}^2(1 + z) \quad (5)$$

This yields

$$\frac{d\Sigma^{-1}}{d\Omega}(Q) = \frac{1 + (R_{g_{D,z}}{}^2(1 + z)Q^2)/3}{(1 - \Phi_D)V_D{}^w(1 + w)\Delta\rho^2} + \frac{1 + (R_{g_{D,z}}{}^2Q^2/3)}{\Phi_D V_D{}^w \Delta\rho^2} \quad (6)$$

where all "hydrogen" terms have been eliminated. Reorganizing terms leads to

$$\frac{d\Sigma^{-1}}{d\Omega}(Q) = \frac{1 - (\Phi_D w/(1 + w))}{\Phi_D(1 - \Phi_D)V_D{}^w\Delta\rho^2} + \frac{(R_{g_{D,z}}{}^2Q^2/3)[1 + (\Phi_D(z - w)/(1 + w))]}{\Phi_D(1 - \Phi_D)V_D{}^w\Delta\rho^2} \quad (7)$$

Now, one can find a simple relationship between z and w. The weight-average $R_{g_w}{}^2$ and z-average $R_{g_z}{}^2$ are connected by the formula[14]

$$R_{g_w}{}^2 = \frac{U + 1}{2U + 1}R_{g_z}{}^2 \quad (8)$$

The same relationship holds for M_w and M_z (in the case of Gaussian coils). Hence

$$1 + z = M_z{}^H/M_z{}^D = \frac{(2U^H + 1)}{(U^H + 1)}\frac{(U^D + 1)}{(2U^D + 1)}\frac{M_w{}^H}{M_w{}^D} = \frac{(2U^H + 1)}{(U^H + 1)}\frac{(U^D + 1)}{(2U^D + 1)}(1 + w) \quad (9)$$

So, if $U^D = U^H$, it follows that $z = w$, and from eq 7 no correction for $R_{g_{D,z}}{}^2$ arises to the first order. For $V_w{}^D$ one obtains a correction factor close to unity for the concentrations considered.

Thus we can eliminate the index D from the formulas. Equation 7 then reduces to the known Zimm form:

$$\frac{d\Sigma^{-1}}{d\Omega}(Q) = \frac{1 + Q^2R_{g_z}{}^2/3}{\Phi(1 - \Phi)V^w\Delta\rho^2} \quad (10)$$

From this equation, the molar mass is extracted from the intercept at $Q = 0$. The slope of $d\Sigma/d\Omega$ vs Q^2 yields the z-average radius of gyration, which transforms into R_{g_w} according to eq 8.

The absolute values for the cross-sections are derived from the measured neutron scattering intensities I^s by calibration to the incoherent scattering from a secondary Lupolen standard, as given elsewhere.[13,15] The incoherent scattering of the protonated matrix material was obtained separately in the experiment and corrected independently. The desired coherent part of the scattering is then given by

$$\frac{d\Sigma}{d\Omega}(Q)^{coh} = \frac{d\Sigma}{d\Omega}(Q)^s - (1 - \Phi_D)(T^s/T^{Mat.})\frac{d\Sigma}{d\Omega}(Q)^{inc} \quad (11)$$

$T^{Mat.}$ is the transmission of the matrix. In the limit of the experimental errors, $T^s/T^{Mat.}$ was set equal to unity.

RIS Theory

The essential feature of the RIS model is that the bond rotational angles ϕ are allowed to accept only a number of discrete values which correspond to minima in the conformational energy.[5,16] The simplest approach is based on a three-state model comprising the trans (t), gauche$^+$ (g^+) and gauche$^-$ (g^-) states, which are related to a rotation of 0°, +120°, and −120°, respectively. Assuming that the rotational potential of bond i depends only upon the rotation of i itself and upon that of neighboring bonds, thus neglecting long-range interactions, one can rearrange the conformational energies such that the energy of bond i is a function characterized by two indexes ζ and ξ. ζ indexes the state of bond $i - 1$; ξ, that of bond i. The corresponding statistical weights $\exp(-E_{\zeta\xi}/RT)$ are collected in a 3 × 3 matrix:

$$\mathbf{U}_i = [u_{\zeta\xi;i}] = [\exp(\zeta\xi;i/RT)] \quad (12)$$

If one knows the statistical weight matrices for every bond i, all conformation-dependent properties of the chain can be calculated in the framework of the RIS theory. By virtue of the monomeric repeat units, the statistical matrices that differ from each other are small in number.

Considering the case of PEP, attention must be paid to the fact that in the experiment we deal with atactic chains. Thus, d and l centers occur with equal probabilities, and an appropriate average has to be performed.[5] For the d configuration we arrive at the expressions for the matrices given by Mark:[1]

$$\mathbf{U}_d = \begin{pmatrix} \eta & 1 & \tau \\ \eta & 1 & \tau\omega \\ \eta & \omega & \tau \end{pmatrix}$$

$$\mathbf{U}_e = \begin{pmatrix} 1 & \sigma & \sigma \\ 1 & \sigma & \sigma\omega \\ 1 & \sigma\omega & \sigma \end{pmatrix}$$

$$\mathbf{U}_{de} = \begin{pmatrix} 1 & \sigma\omega & \sigma \\ 1 & \sigma & \sigma\omega \\ 1 & \sigma\omega & \sigma\omega \end{pmatrix}$$

$$\mathbf{U}_{ed} = \begin{pmatrix} \eta & \tau & 1 \\ \eta & \tau\omega & \omega \\ \eta\omega & \tau\omega & 1 \end{pmatrix}$$

We have used the suggested indexes for the matrices

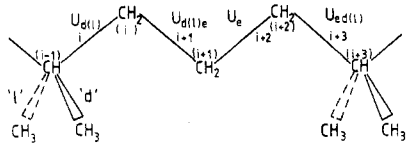

Figure 1. Schematic of the PEP chain.

proposed by Mark.[1] The corresponding bonds are shown in Figure 1.

The parameters σ and ω are related to three and four bond interactions, respectively. Their values have been determined by spectroscopic measurements of short alkane homologues[17,18] and by calculations using a semiempiric interaction potential.[19] η and τ result from the sterically nonequivalent interactions of the CH, CH_2, and CH_3 groups and from geometrical considerations. For the approximation that all groups are sterically equivalent, $\eta = 1$. τ is the statistical factor assigned to the syn conformation of CH_3 and CH. τ and η are connected by σ:

$$\tau = \sigma\eta \tag{13}$$

Hence, only three statistical parameters σ, ω, and τ differ from each other. The matrices of the l configuration are obtained by a simple interchange of both the second and third rows and the second and third columns of the corresponding d matrices.

With the help of the above matrices, the partition function is written:[5]

$$\mathbf{Z} = \mathbf{J}^*[\prod_{i=2}^{n-1}\mathbf{U}_i]\mathbf{J} \tag{14}$$

where n is the number of bonds, $\mathbf{J}^*$ the row vector consisting of one unity and two zeros, and $\mathbf{J}$ the column vector solely consisting of unities. The characteristic ratio is given by[5]

$$C_n = \langle R^2\rangle_0/nl^2 = 2(\mathbf{Z}nl^2)^{-1}\mathcal{J}^*[\prod_{i=1}^{n}\mathcal{G}_i]\mathcal{J} \tag{15}$$

where $\mathcal{J}^*$ is the row vector consisting of a single unity followed by 14 zeros and $\mathcal{J}$ the column vector consisting of 12 zeros followed by 3 unities. The $\mathcal{G}_i$ are the *generator* matrices. They are given by

$$\mathcal{G} = \begin{pmatrix} \mathbf{U} & (\mathbf{U}\otimes l^{\mathrm{T}})\|\mathbf{T}\| & l^2\mathbf{U} \\ 0 & (\mathbf{U}\otimes \mathbf{E}_3)\|\mathbf{T}\| & \mathbf{U}\otimes l \\ 0 & 0 & \mathbf{U} \end{pmatrix} \tag{16}$$

The symbol $\otimes$ designates the direct matrix product. l^{T} and l are the transpose and magnitude, respectively, of the skeletal bond vector. The matrix $\|\mathbf{T}\|$ is a pseudodiagonal matrix defined by

$$\|\mathbf{T}\| = \begin{pmatrix} \mathbf{T}(\phi_t) & & \\ & \mathbf{T}(\phi_{g^+}) & \\ & & \mathbf{T}(\phi_{g^-}) \end{pmatrix} \tag{17}$$

The elements $\mathbf{T}(\phi_i)$ are the transfer matrices $\mathbf{T}_i$, which transform a vector given in the coordinate system $i+1$ into that of system i.[5]

Owing to the fact that rotations about the first and the last bond of the chain are not specified, the statistical matrices in $\mathcal{G}_1$ and $\mathcal{G}_n$ are simply given by $\mathbf{E}_3$, the unit matrix of order three.

The four statistical matrices as well as the generator matrices for one monomeric unit containing a d or l center were combined into one matrix in order to reduce the number of matrix multiplications in eq 15.

$$\mathbf{U}_{\mathrm{D}} = \mathbf{U}_{\mathrm{e}}\mathbf{U}_{\mathrm{ed}}\mathbf{U}_{\mathrm{d}}\mathbf{U}_{\mathrm{de}} \tag{18}$$

$$\mathbf{U}_{\mathrm{L}} = \mathbf{U}_{\mathrm{e}}\mathbf{U}_{\mathrm{el}}\mathbf{U}_{\mathrm{l}}\mathbf{U}_{\mathrm{le}} \tag{19}$$

The same order holds for the generator matrices. The stereochemical sequence of d and l centers was generated by a set of random numbers assigning a d center to the occurrence of a number <0.5 and an l center to a number >0.5.

The directly accessible quantity in the experiment is the radius of gyration. For the comparison of theory and experiment, R_g was calculated from C_n according to the Debye relation which is strictly valid in the $\lim_{n\to\infty}$:

$$R_g = ((C_\infty/6)n_b N l^2)^{1/2} \tag{20}$$

where N denotes the number of monomeric units, n_b is the average number of bonds per monomeric unit, l is the average bond length, and C_n is the characteristic ratio given by eq 15. The number of bonds n is given by $n_b N$.

The differential temperature coefficients may be evaluated using eq 15:

$$\kappa = \frac{\partial \ln C_\infty}{\partial T} = \frac{1}{\langle R^2\rangle_0}\frac{\partial\langle R^2\rangle_0}{\partial T} \tag{21}$$

The derivation of $\langle R^2\rangle_0$, the root mean square end-to-end distance, involves the calculation of $\partial\mathbf{Z}/\partial\mathbf{T}$ and $(\partial/\partial\mathbf{T})(\prod_i\mathcal{G}_i)$.

These are performed following an idea outlined by Flory which involves "hypermatrices":[5]

$$\hat{\mathbf{U}}_i = \begin{pmatrix} \mathbf{U}_i & \partial\mathbf{U}_i/\partial\mathbf{T} \\ 0 & \mathbf{U}_i \end{pmatrix}$$

$$\hat{\mathcal{G}}_i = \begin{pmatrix} \mathbf{U}_i & \partial\mathcal{G}_i/\partial\mathbf{T} \\ 0 & \mathcal{G}_i \end{pmatrix}$$

where $\partial\mathcal{G}_i/\partial\mathbf{T}$ and $\partial\mathbf{U}_i/\partial\mathbf{T}$ are the derivatives of all elements of the matrices with respect to temperature. One obtains

$$\kappa = \frac{2}{\langle R^2\rangle_0\mathbf{Z}^2}\Big[\mathcal{J}_{15}^*\frac{\partial}{\partial\mathbf{T}}(\prod_{i=1}^{n}\mathcal{G}_i)\mathcal{J}_{15}\mathbf{Z} - \frac{\partial\mathbf{Z}}{\partial\mathbf{T}}\mathcal{J}_{15}^*(\prod_{i=1}^{n}\mathcal{G}_i)\mathcal{J}_{15}\Big] = \frac{2}{\langle R^2\rangle_0\mathbf{Z}^2}[\mathcal{J}_{30}^*(\prod_{i=1}^{n}\mathcal{G}_i)\mathcal{J}_{30}\mathbf{Z} - \mathcal{J}_6^*(\prod_{i=2}^{n-1}\hat{\mathbf{U}}_i)\mathcal{J}_6\mathcal{J}_{15}^*(\prod_{i=1}^{n}\mathcal{G}_i)\mathcal{J}_{15}] \tag{22}$$

The influence of bond- or valence-angle fluctuations is introduced using the technique described by Cook and Moon.[20] In their model the rotational (or valence) angles oscillate in potential wells about the RIS minima for each bond. Assuming that the fluctuations of different angles do not interfere, the transformation matrices $\mathbf{T}_i$ can be averaged for δ_ϕ independently.

$$\langle\mathbf{T}_i\rangle_f = \begin{pmatrix} \langle\cos\theta\rangle & \langle\sin\theta\rangle & 0 \\ \langle\sin\theta\rangle\langle\cos\theta\rangle & -\langle\cos\theta\rangle\langle\cos\phi\rangle & \langle\sin\phi\rangle \\ \langle\sin\theta\rangle\langle\sin\phi\rangle & -\langle\cos\theta\rangle\langle\sin\phi\rangle & -\langle\cos\phi\rangle \end{pmatrix} \tag{23}$$

with

$$\langle\cos\phi\rangle = (\cos\phi_0)\exp(-\delta_\phi^2/2) \tag{24}$$

$$\langle\cos\theta\rangle = (\cos\theta_0)\exp(-\delta_\theta^2/2) \tag{25}$$

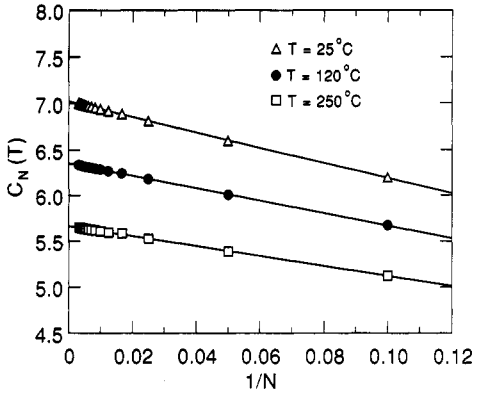

Figure 2. C_N vs $1/N$, extrapolation to C_∞.

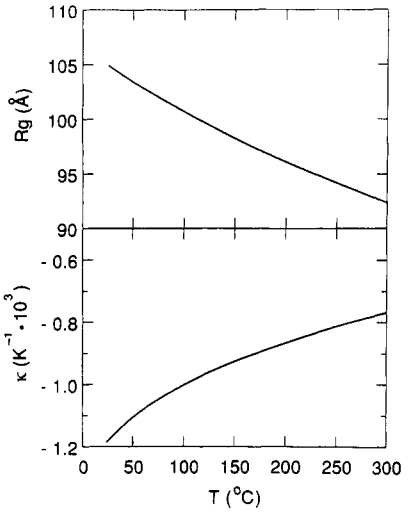

Figure 3. RIS results for radius of gyration R_g, differential temperature coefficient κ.

and in an analogous fashion for the sine terms.

Results

For the initial calculation we used the parameters given by Mark,[1] where $\phi_t = 0°$, $\phi_{g^+,g^-} = 120°$, $\theta = 68°$, $l = 1.54$ Å, $E_\sigma = 500$ cal/mol, $E_w = 2000$ cal/mol, τ(room temp) = 0.43, and $\eta = 1$. The values of the statistical weights at different temperatures were calculated on the assumption that each could be expressed as a Boltzmann factor in the conformational energy. The conformational average was taken over five chains. This turned out to be sufficient as the characteristic ratio is not very sensitive to the stereochemical sequence. Like all conformation-dependent properties, in the RIS model, the characteristic ratio depends on the number of bonds n or monomers N used in the calculation. To yield the saturation value in the limit of $N \rightarrow \infty$, C_N was plotted vs. $1/N$. C_∞ was extrapolated by linear regression. The plots for three different temperatures are shown in Figure 2.

Altogether, 15 temperatures in the range of 25–280 °C were investigated. R_g has been calculated from C_∞ using eq 20. The results are displayed in Figure 3. The corresponding values are listed in Table I. The differential temperature coefficients were similarly evaluated by linear regression, as described above. $\kappa(T)$ is also shown in Figure 3. One observes a steady decrease of C_∞, or R_g, respectively, but not strictly linearly, as the shrinkage of κ with T suggests.

In the experiment, the temperature was varied in steps of about 30 °C from room temperature to 270 °C. The samples and the hydrogenated matrix were calibrated separately and corrected for background noise. The coherent cross-sections were obtained using eq 11. The transmissions, the density (and hence the contrast factors), and the incoherent scattering depend on temperature. Thus the transmissions of all samples and the matrix were measured at least at every second temperature. The matrix showed a flat background except for the small Q range, where a weak peak was observed for the aforementioned reason. In this regime the data were fitted by a parabola, while at higher Q values they were simply averaged. Due to inelastic processes the incoherent intensity slightly rises with temperature.

Table I
Radii of Gyration Determined by RIS Theory and Experiment

T/°C	R_g^{RIS}/Å	$R_{g_{w,6\%}}$/Å	$R_{g_{w,4\%}}$/Å	$R_{g_{w,2\%}}$/Å	$R_{g_{w,av}}$/Å
25	105.0	107.5 ± 0.6	105.9 ± 0.5	105.6 ± 0.4	106.1 ± 0.3
50	103.5				
55		105.3 ± 0.6	104.4 ± 0.2	104.3 ± 0.2	104.4 ± 0.2
80	101.8	103.1 ± 0.4	103.3 ± 0.2	102.1 ± 0.6	103.2 ± 0.2
100	100.8				
120	99.8	99.8 ± 0.2	101.3 ± 0.3	99.7 ± 0.2	100.0 ± 0.2
150	98.4	99.6 ± 0.6	99.8 ± 0.3	98.1 ± 0.3	99.0 ± 0.2
180	97.1	97.4 ± 0.4	98.2 ± 0.5		97.7 ± 0.3
200	96.3		99.3 ± 0.2	97.7 ± 0.7	99.2 ± 0.2
210	95.8	98.4 ± 0.6	98.6 ± 0.4		98.4 ± 0.5[a]
215				98.4 ± 0.9	
220	95.4				
227			97.9 ± 0.2		97.9 ± 0.2
240	94.7	96.3 ± 0.2			96.0 ± 0.2[b]
250	94.3				
260	93.9	95.3 ± 0.3			95.3 ± 0.3
270	93.5		96.3 ± 0.4		96.3 ± 0.4
280	93.2				

[a] Value averaged from 210 and 215 °C. [b] Value averaged from 240 and 245 °C.

All quantities mentioned above were extrapolated linearly at the temperatures which were not measured. Figure 4 displays the calibrated and corrected data for the three concentrations at two different temperatures. The corresponding Debye fits are also shown.

In order to give the qualitative behavior of $R_g(T)$, we have plotted the data in the Zimm format (eq 10) but here as $S(Q)^{-1}$ vs Q^2. $S(Q)$ and $d\Sigma/d\Omega$ are related simply by a constant:

$$\frac{d\Sigma}{d\Omega}(Q)\frac{N_A}{\Delta\rho^2} = S(Q) \tag{26}$$

This form has the advantage that the neutron scattering dependent quantity $\Delta\rho^2$ is eliminated. In Figure 5, the 6% sample data are plotted for four temperatures. The decreasing slopes illustrate the shrinkage of R_g with temperature. The plots also serve to show the quality of absolute calibration by calculation of M_w from the intercept at $Q = 0$. The results are listed in Table II. They are to be compared with the light scattering value of $M_w = 8.22 \times 10^4$ g/mol. The 6 and 4% samples show good agreement within the experimental error; the 2% sample seems to have a smaller value. We attribute this deviation to uncertainties in the absolute calibration factors. Post-SANS SEC measurements showed no change in M_w/M_n over the experimental temperature range.

For a quantitative evaluation of the data, one has to look for a possible nonzero χ parameter between hydrogenated and deuterated chains. Evidence for a nonvanishing interaction parameter in isotope mixtures was found by Bates et al.[21] and Schwahn et al.[22] In this case, eq 10

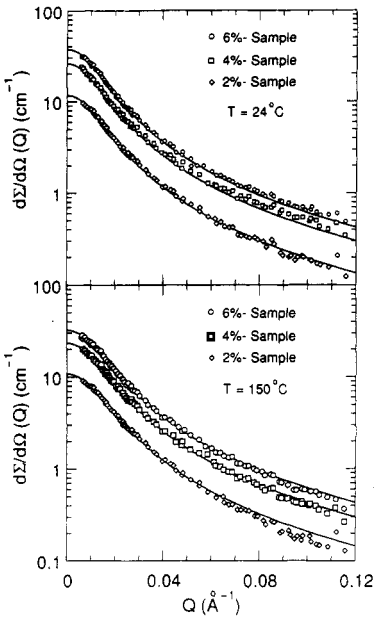

Figure 4. Experimental spectra for the three concentrations at two temperatures, corresponding Debye fits.

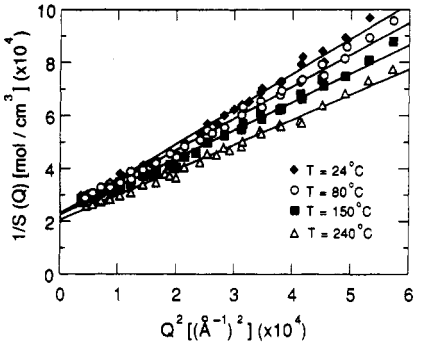

Figure 5. Zimm plots of the 6% sample data at various temperatures.

Table II
Weight-Average Molar Masses by SANS for the Investigated Samples at Different Temperatures

T/°C	$M_{w,6\%}$/(g/mol)	$M_{w,4\%}$/(g/mol)	$M_{w,2\%}$/(g/mol)
24	84 400 ± 1000	87 400 ± 500	74 200 ± 500
80	81 100 ± 500	87 100 ± 500	76 500 ± 600
150	80 400 ± 1000	82 300 ± 500	73 200 ± 1000
240	81 100 ± 1000	78 300 ± 1000	

has to be modified:

$$\frac{1}{S(Q)} = \frac{1 + Q^2 R_{g_z}{}^2/3}{\Phi(1-\Phi)V^w} - 2\chi \qquad (27)$$

Here, χ is measured in mol/cm³ and V^w in cm³/mol. Following a procedure analogous to that used for the determination of second virial coefficients in light scattering,[23] we have plotted $\Phi(1-\Phi)/S(Q)$ vs $Q^2 + \Phi(1-\Phi)c$, where c is an arbitrary constant. Extrapolating $Q \to 0$, χ can be determined from the slope in Φ. The plots are displayed in Figure 6, again for 24 and 150 °C. Obviously the χ parameter seems to be very small; the $Q = 0$ slopes are close to zero. The χ values for three temperatures are $(-5.2 \pm 4.0) \times 10^{-6}$ (24 °C), $(-2.4 \pm 4.2) \times 10^{-6}$ (120 °C), and (-3.8 ± 4.0) mol cm⁻³ (150 °C). The absolute values and the corresponding errors are of the same magnitude. This is a problem of absolute calibration for which χ is very sensitive. To examine the interaction parameter more exactly, additional concentrations have to be measured

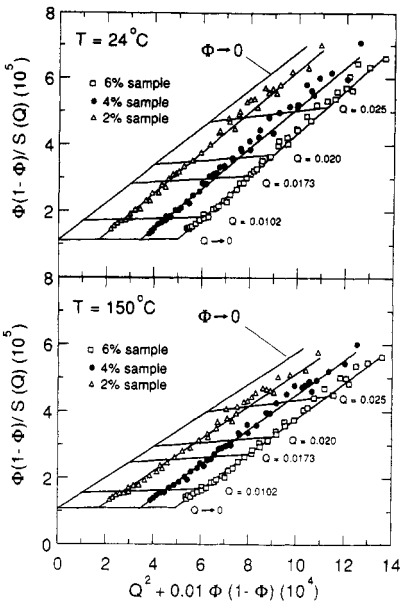

Figure 6. Concentration-dependent Zimm plots at two temperatures.

and better absolute calibration is required. Because of the small absolute values and the large errors, χ was set equal to zero in the evaluation of the data.

To extract $R_g(T)$ from the Zimm plot, one has to make sure that the condition $QR_g < 1$ is fulfilled. Otherwise, the Zimm analysis yields inflated values for R_g. Because the above restriction was not valid in most of the Q range measured, we evaluated the data using the Debye function according to eq 1 in the simplified form:

$$\frac{d\Sigma}{d\Omega}(Q) = \Phi(1-\Phi)\Delta\rho^2 V^w g_D(z)$$
$$= \frac{d\Sigma}{d\Omega}(0)\, g_D(z) \qquad (28)$$

The forward scattering $d\Sigma/d\Omega(0)$ and R_g were used as fitting parameters in the analysis. The Debye fits are shown in Figure 4. $R_g(T)$ was extracted for all concentrations independently. The values were then averaged at the temperatures where two or three concentrations had been measured. The final results are listed in Table I.

Discussion and Conclusion

Both the RIS model and the experimental data reveal a radius of gyration R_g or a characteristic ratio C_∞ which decreases with increasing temperature. Figure 7 compares the RIS results with the experimental ones. The general temperature dependence of both quantities is very similar: At low and intermediate temperatures both decrease with a nearly identical temperature coefficient ($\kappa_{RIS} \simeq -1.1 \times 10^{-3}$ K⁻¹ (refs 1 and 4) and $\kappa_{SANS} = (-1.16 \pm 0.03) \times 10^{-3}$ K⁻¹ (this work)), which within the errors also agrees with the Θ solvent value of $(-1 \pm 0.2) \times 10^{-3}$ K⁻¹ deduced from viscosity experiments. Above 180 °C both sets of data exhibit clear deviations from a constant-temperature coefficient, a phenomenon being more pronounced for the experimental data. The absolute values of R_g resulting from the RIS calculations are slightly below the experimental values. Below about 180 °C the average deviation is on the order of 1%; at higher temperatures it increases to about 2–3%. We wish to emphasize that this very good agreement was achieved without any adjustable parameter. We further note that the increasing discrepancy at higher temperatures appears to be a systematic effect indicating

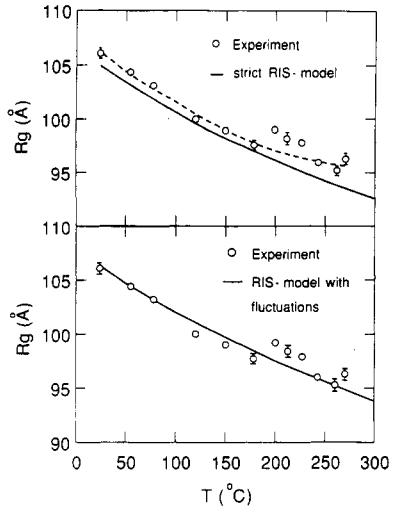

Figure 7. Comparison of experimental and theoretical results for the radii of gyration R_g in the strict RIS model, comparison considering fluctuations. The dashed line in the upper part of the figure is for guiding the eyes.

that the sterical hindrance at higher temperatures becomes more important than the RIS model assumes. Several effects may play a role.

(i) As with increasing temperature the gauche conformations are more and more occupied, the direct steric interactions between the methyl side groups, which are neglected in the four-bond interaction approach of the RIS ansatz, may come into play.

(ii) The presence of about 18 isopropyl side chains per 1000 backbone carbons may also exert an influence on the chain conformation by hindering the attenuation of coil size.

In order to try to improve the already very good agreement we varied the bond energies and explicitly took into account bond angle fluctuations in a harmonic approximation. The fluctuations were calculated from the rotational potential given by Rigby and Roe:[24]

$$U(\cos\phi) = \sum_{n=0}^{5} a_n \cos^n \phi \qquad (29)$$

where the a_i are experimentally determined parameters. In the "trans well" we estimate the fluctuations by a harmonic approximation:

$$U(\phi) = 1/2k\phi^2 \qquad (30)$$

where k is given by $\partial^2 U/\partial\phi|_{\phi=t}$. k is calculated to be 73 kJ/mol. Using this value we estimate $\Delta\phi = 9.5°$ for the zero point fluctuation at $T = 0$ K. Performing the thermal average the temperature dependence of the fluctuations can be written in the form:

$$\Delta\phi(T) = \Delta\phi(T{=}0)\left(\coth\frac{\hbar\omega}{2k_BT}\right)^{1/2} \qquad (31)$$

$\hbar\omega$ was calculated from the ground-state energy which is approximately 2 kJ/mol.[25] For the valence angle fluctuation $\Delta\theta = 3°$ was introduced. The best values for the bond parameters were found to be $E_\sigma = 600$ cal/mol and $E_w = 2400$ cal/mol while η was kept to unity. These values are within the experimental error of the bond energy determination. With these bond energies together with the angular fluctuations we arrive at the solid line in the lower part of Figure 7. Excellent agreement in absolute values and temperature coefficients is achieved at lower T. At higher temperatures the experimental data appear to suggest a somewhat larger bending than the theoretical curve predicts. However, within the experimental accuracy, the theoretical curve provides a very good, if not excellent, interpolation of the experimental results. The introduction of angle fluctuations is a more realistic approach. Hence the consonance of the curves shows that the "new" values for the bond energies E_σ and E_ω are more appropriate for describing the internal rotational potentials of the PEP chain.

Measuring the temperature-dependent chain dimensions of PEP in the melt over a large temperature range, we tried to scrutinize the RIS concept beyond what has been attempted so far.

(i) Examining the melt instead of Θ solvents we definitely avoided residual solvent effects, which could play a role in comparison of chain dimensions obtained in different Θ solvents at different temperatures.

(ii) Covering a large temperature range for the first time, we were able to test the intramolecular potentials beyond a determination of a constant-temperature coefficient.

The experimental results are in remarkable agreement with Θ solvent data, concerning both temperature coefficient and absolute magnitude of $\langle R_g\rangle/M^{1/2}$. Over the common temperature range (25.0 °C < T < 60.9 °C) the $\langle R_g\rangle/M^{1/2}$ values deduced from neutron scattering vary between 3.97×10^{-2} and 3.88×10^{-2} nm while the Θ solvent results give 3.81×10^{-2} and 3.72×10^{-2} nm, an agreement in absolute R_g terms of about 4%. This points out that residual solvent effects in the viscosity data from Θ solvents are, if at all, very small. It also shows the accuracy of the Flory–Fox hydrodynamic interaction parameter $\Phi_0 = 2.5 \times 10^{21}$. Vice versa, it further indicates that deviations from ideality due to local interchain interactions in the melt are not important, a conclusion previously reached by Yoon and Flory[26] for oligomeric polyethylene.

Note Added in Proof. SANS chain dimension measurements of polyethylene melts have been reported: Boothroyd, A. T.; Rennie, A. R.; Boothroyd, C. B. *Europhys. Lett.* **1991**, *15*, 715. Over the temperature range of 110–210 °C, κ was found to be -1.5×10^{-3} K^{-1}, a value in excellent agreement with RIS predictions and that from the Θ condition and athermal solvent measurements.

Acknowledgment. We thank Professor N. Hadjichristidis, University of Athens, for the characterization of the PEP samples and G. Pohl and U. Bünten for their valuable technical assistance.

References and Notes

(1) Mark, J. E. *J. Chem. Phys.* **1972**, *57*, 2541.
(2) Brückner, S.; Allegra, G.; Gianotti, G.; Moraglio, G. *Eur. Polym. J.* **1974**, *10*, 347.
(3) Allegra, G. *Makromol. Chem.* **1968**, *117*, 12.
(4) Mathur, S. C.; Mattice, W. H. *Makromol. Chem.* **1988**, *189*, 2893.
(5) Flory, P. J. *Statistical Mechanics of Chain Molecules*; Wiley: New York, 1969.
(6) Flory, P. J.; Ciferri, A.; Chiang, R. *J. Am. Chem. Soc.* **1961**, *83*, 1023.
(7) Flory, P. J.; Fox, T. G. *J. Am. Chem. Soc.* **1951**, *73*, 1904, 1909, 1915.
(8) Mays, J. W.; Fetters, L. J. *Macromolecules* **1989**, *22*, 921.
(9) de Gennes, P. G. *Scaling Concepts in Polymer Physics*; Cornell University Press: Ithaca, NY, 1979.
(10) Fetters, L. J.; Hadjichristidis, N.; Mays, J. W. *Macromolecules* **1984**, *17*, 2723.
(11) Fetters, L. J.; Hadjichristidis, N.; Xu, Z.; Roovers, J. *J. Polym. Sci., Pol. Phys. Ed.* **1982**, *20*, 743.
(12) *Experimentiereinrichtungen im Forschungsreaktor und im Neutronenleiterlabor*; Forschungszentrum Jülich: Jülich, Germany, 1986.

(13) Pyckhout-Hintzen, W.; Springer, T.; Forster, F.; Gronski, W.; Frischkorn, C. *Macromolecules* **1991**, *24*, 1269.
(14) Brandup, J.; Immergut, E. H. *Polymer Handbook*, 2nd ed.; Wiley: New York, 1975; p IV-310.
(15) Wignall, G. D.; Bates, F. S. *J. Appl. Crystallogr.* **1987**, *20*, 28.
(16) Volkenstein, M. V. *Configurational statistics of polymeric chains*; Interscience: New York, 1963.
(17) Mizushima, S. *Structure of molecules and internal rotations*; Academic Press: New York, 1954.
(18) Person, W. B.; Pimentel, G. C. *J. Am. Chem. Soc.* **1953**, *75*, 532.
(19) Abe, A.; Jernigan, R. L.; Flory, P. J. *J. Am. Chem. Soc.* **1966**, *88*, 631.
(20) Cook, R.; Moon, M. *Macromolecules* **1980**, *13*, 1537.
(21) Bates, F. S.; Dierker, S. B.; Wignall, G. D. *Macromolecules* **1986**, *19*, 1938.
(22) Schwahn, D.; Hahn, K.; Springer, T. *J. Chem. Phys.* **1990**, *93*, 11.
(23) Higgins, J. S. *Polymer Conformations and Dynamics*; Treatise on Materials Science and Technology; 15; Academic Press: New York, 1979.
(24) Rigby, D.; Roe, R. J. *J. Chem. Phys.* **1987**, *87*, 7285.
(25) Streitwieser, A.; Heathcock, C. H. *Introduction to Organic Chemistry*; Macmillan: New York, 1976.
(26) Yoon and Flory (Yoon, D. Y.; Flory, P. J. *J. Chem. Phys.* **1978**, *69*, 2526) used 600 cal/mol for the first-order interaction energy in their RIS-based evaluation of *n*-alkane chains, *n*-$C_{16}H_{34}$ and *n*-$C_{36}H_{74}$. Therein, the melt- and solution-based R_g SANS results of Dettenmeier (Dettenmeier, M. *J. Chem. Phys.* **1978**, *68*, 2319) and the RIS predictions coincide when E_σ of 600 cal/mol is used. The range of values considered for E_σ was 500–1000 cal/mol.